Structure of monolayer Ar on Pt(111): Possible realization of a devil's staircase in two dimensions

Peter Zeppenfeld, Ulrich Becher, Klaus Kern,* and George Comsa
Institut für Grenzflächenforschung und Vakuumphysik, KFA Forschungszentrum Jülich, Postfach 1913, D-5170 Jülich, Germany
(Received 22 July 1991; revised manuscript received 8 November 1991)

The structure of Ar physisorbed on Pt(111) in the submonolayer-coverage regime has been explored by thermal He-atom scattering. On the clean Pt(111) surface Ar condenses in a hexagonal close-packed phase aligned with the substrate. At coverages $\Theta \lesssim 0.7$ ML the Ar adlayer lattice parameter is about 3.81 Å. When the Ar coverage increases above 0.75 ML a first-order phase transition into a compressed hexagonal Ar phase with a lattice constant of 3.70 Å is observed. From thermal-expansion measurements and the appearance of superlattice diffraction peaks, the compressed phase is demonstrated to be a high-order commensurate phase, characterized by a $(4\times4)R0°$ commensurate unit cell containing nine argon atoms. We have found experimental evidence for further high-order commensurate phases also in the low-Ar-coverage regime. Therefore the phase diagram of the Ar/Pt(111) physisorption system is likely to be a realization of a *devil's staircase* in two dimensions.

I. INTRODUCTION

The investigation of physisorbed rare-gas adlayers has been shown to provide a powerful tool for the understanding of elementary processes of interest in surface science, such as adsorption and desorption, surface melting, and wetting.[1] In addition, physisorption systems have acquired model character in the study of structural and dynamical properties of adsorbed layers and thin films.[2]

In a simplified picture the structure of an adsorbed layer is governed by the competition between the lateral adatom-adatom interaction h and the surface corrugation potential u_c of the underlying substrate that the adatom is subject to. On the one hand, the lateral interaction between the adatoms will tend to establish an adlayer structure determined by the natural adlayer interatomic distance, i.e., incommensurate with the substrate. On the other hand, the lateral variation of the substrate-adatom potential (corrugation) will try to force the adatoms to occupy energetically favored adsorption sites, hence leading to a commensurate structure. In the case where the lateral adatom interaction and the corrugation of the adatom-substrate potential have about equal magnitude, $h/u_c \simeq 1$, the adlayer structure (commensurate versus incommensurate) will largely depend on the structure's symmetries and the ratio of the lattice constants of adlayer and substrate, as well as on the actual physical conditions (such as coverage, spreading pressure, and surface temperature). Varying these conditions, structural phase transitions between different commensurate and incommensurate phases may occur and complex phase diagrams can be obtained as, for instance, in the case of physisorbed rare gases on graphite[3] and metal surfaces.[2]

In the past 10 years, phase diagrams and phase transitions of a large number of physisorption systems have been studied.[4,5] Also, much theoretical effort has been devoted to describe the different phases and phase transitions. For instance, the commensurate-incommensurate (C-I) phase transition has been explained in terms of domain-wall formation.[6] Depending on the interaction between domain walls, either striped or hexagonal domain-wall patterns will result; the nature of the corresponding C-I phase transitions will be completely different (second or first order, respectively).[7] These theoretical predictions have been verified experimentally for a variety of different systems.[8]

Another interesting concept describing structural phase transitions of adsorbed layers has been developed by Aubry.[9] The basic idea is that any adlayer structure incommensurate with the substrate can be approximated within any given accuracy by a so-called high-order commensurate (HOC) structure. These HOC structures are characterized by a (large) commensurate unit cell hosted by several adlayer atoms. Since a fraction of the adatoms will always lock onto preferential adsorption sites, these HOC (locked) phases should be energetically favored with respect to a true incommensurate (floating) phase. If the corrugation potential is sufficiently large, it is expected that the phase diagram of the adlayer is composed of several HOC phases. The corresponding (first-order) phase transitions will involve discrete jumps of the interatomic distance moving from one HOC phase to the other. Such a stepwise variation of the lattice parameter within a sequence of HOC phases is called a "devil's staircase."[9] Of course, this simple picture is modified at higher surface temperatures where thermal fluctuations become important and will destabilize those HOC phases with large unit cells.

We have demonstrated earlier[10] that one can distinguish experimentally between a locked HOC phase (where the ratio between the interatomic distances of the adsorbate and substrate is a rational number) and a floating incommensurate phase (where this ratio is an irrational number). We have proposed two criteria based on the thermal expansion and adlayer superstructure, respectively, which allow a qualitative distinction between

a HOC and an incommensurate phase.

(1) The thermal expansion of an incommensurate floating rare-gas adlayer is expected to be similar to that of the corresponding bulk crystal, whereas the locked HOC phase has to follow the thermal expansion of the underlying substrate to which it is locked. Since the thermal-expansion coefficients of rare-gas solids are at least 10 times larger than those of the substrates normally used, a distinction between HOC and incommensurate phases becomes straightforward. Of course, this criterion requires that the temperature range in which the HOC phase is stable with respect to thermal fluctuations is large enough ($\gtrsim 10$ K) to allow a reliable thermal-expansion measurement.

(2) The locking of the adlayer into a HOC phase leads to a periodic modulation of the adlayer with the periodicity determined by the commensurate unit cell of the HOC phase. This modulation should give rise to superlattice diffraction peaks, which are absent in the incommensurate floating phase. From the superlattice diffraction pattern, the commensurate unit cell of the adlayer HOC phase can be determined.

Following these criteria, we were able to demonstrate the existence of a HOC phase and the corresponding *I*-HOC phase transition on Kr physisorbed on Pt(111).[10] Recently, with use of the same criteria, HOC phases have also been found in CF_3CI monolayers on graphite and Ar on MgO(100).[11] For the latter system, model potential calculations performed by Girard and Girardet yield a minimum energy for the $(2\times 3)R0°$ HOC phase, in agreement with the experimental results. HOC phases have also been found in chemisorbed systems such as Pb/Cu(110).[12]

Now that HOC phases have been shown to really exist and since they can be experimentally accessed, it is interesting to search for a possible realization of a devil's staircase, i.e., for HOC-HOC transitions in physisorbed adlayers. It has been shown by Steele[13] and Vidali and Cole[14] that on the same substrate (in their case, graphite) the *absolute* value of the corrugation energy u_c increases with the size of the rare-gas adatom; however, it *decreases* relative to the binding energy of the adatom as well as relative to the lateral interaction energy h between the adatoms (i.e., the ratio h/u_c increases from Ar to Xe): "this familiar conclusion[13] follows because a larger adatom 'sees' a smoother surface all the rest being the same" (Ref. 14, p. 6737). Thus, within this simple picture of the competition between lateral interaction and corrugation energy, stable HOC phases and a devil's staircase are most likely to be expected with the lighter rare-earth gases. It is therefore a main motivation and a natural extension of our previous studies of Xe and Kr adlayers on Pt(111) to investigate the structural behavior of Ar physisorbed on the Pt(111) substrate.

II. EXPERIMENT

The results reported below have been obtained with the high-resolution UHV He-atom-scattering apparatus described in detail Ref. 15. The apparatus has been designed for elastic- and inelastic-scattering experiments. In the present context only elastic He diffraction measurements are reported.

The supersonic He-atom nozzle beam is generated by expanding high-purity He gas at high pressure (150 bars) through an orifice with a diameter of ~ 5 μm. By cooling the nozzle with liquid nitrogen, a He beam with an energy of 18.3 meV and an energy spread of 0.25 meV [full width at half maximum (FWHM)] is obtained. The highly monochromatic He beam is directed on the sample, and the scattered He atoms are detected by means of a quadrupole mass analyzer. The He-atom generator and detector being immobile, the total scattering angle is fixed ($\vartheta_i+\vartheta_f=90°$). The scattering conditions are varied by rotating the sample crystal around an axis normal to the scattering plane. In this way the wave-vector transfer parallel to the surface is varied according to

$$Q=k_i(\sin\vartheta_i-\sin\vartheta_f)=\sqrt{2}k_i\sin(\vartheta_i-45°)\ .$$

The angular divergences of the incident beam and angle subtended by the detector are both 0.2°. Together with the energy spread of the incident beam of 0.25 meV, an overall wave-vector resolution $\Delta Q\sim 0.01$ Å^{-1} is obtained. Besides the polar rotation, the sample can also be rotated around its surface normal. This rotation changes the azimuthal orientation of the sample, but leaves the polar angle and wave-vector transfer unchanged.

The sample is a high quality Pt(111) surface with an average terrace width of $\gtrsim 2000$ Å.[16] The surface was cleaned *in situ* by repeated cycles of heating in oxygen and annealing at about 1000 K until no surface impurities could be detected in the Auger spectrum. By Ar^+-ion bombardment and subsequent annealing prior to the measurements, a clean and smooth Pt(111) surface is obtained, which stays free from contamination over several hours even at low surface temperatures (residual pressure in the 10^{-11}-mbar range). This has been checked by monitoring the He-atom reflectivity, which presents a sensitive measure of the cleanliness and smoothness of surfaces.[17]

The Ar adlayers investigated here were obtained by exposing the Pt surface at low temperature (typically 20 K) to an Ar pressure of about 5×10^{-8} mbar. When the desired coverage was reached, the Ar pressure was pumped off and the Ar adlayer was carefully annealed at ~ 35 K. The Ar coverage is obtained by monitoring the He reflectivity with exposure time at constant Ar pressure. This is exemplified in Fig. 1 for an Ar pressure of 7.3×10^{-8} mbar and a surface temperature $T=22$ K. The specularly reflected intensity ($\vartheta_i=\vartheta_f$) continuously decreases with exposure; the starting value I_0 measures the high He reflectivity of the bare Pt(111) substrate. During the exposure, Ar atoms are adsorbed on the surface and nucleate into two-dimensional (2D) islands covering more and more of the Pt surface. In view of the low temperature, the 2D argon-vapor pressure is negligible so that the Pt(111) areas not covered by Ar islands still have the reflectivity of the clean surface. Since the He reflectivity is much smaller for the Ar islands than for the Pt(111) surface (as can be seen in Fig. 1 from the small He intensity at large exposure time), the specular

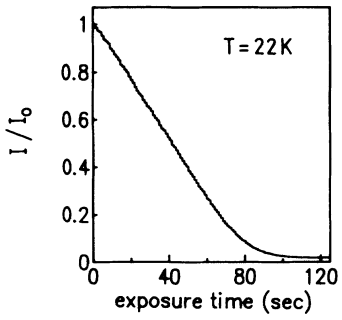

FIG. 1. Specularly reflected He intensity vs Ar exposure. Surface temperature $T=22$ K, Ar pressure $p_{Ar}=7.3\times10^{-8}$ mbar.

He intensity drop is a direct measure of the total area of the Ar islands, i.e., of the Ar coverage: $I/I_0=(1-\Theta)$. Here $\Theta=1$ corresponds to full monolayer (ML) Ar coverage. Thus, from reflectivity curves such as the one in Fig. 1, we are able to calibrate the coverage against exposure with an estimated error of a few percent. From the nearly linear segment observed in Fig. 1, it can be concluded that the Ar sticking coefficient does not change significantly with coverage up to $\Theta\simeq0.8$–0.9 ML. As expected, changing the Ar pressure in the range from 10^{-9} to 10^{-7} mbar has no measurable effect on the sticking coefficient. Adsorption of Ar at higher surface temperature, however, leads to more complex reflectivity curves. The growth of the total area of the Ar islands is then obscured by the Ar 2D gas-solid phase transition[5] and the structural phase transitions in the Ar 2D solid, which will be discussed below.

III. RESULTS AND DISCUSSION

In Fig. 2 a polar He diffraction profile of 0.3 ML Ar physisorbed on a Pt(111) surface is shown. The Ar adlayer was prepared as described above and annealed at 35 K. The spectrum was taken along the $\bar{\Gamma}\bar{M}$ azimuth of the substrate (i.e., along the Pt$\langle 11\bar{2}\rangle$ direction in real space). Since the Pt surface is only partially covered with argon, the first-order Pt diffraction peak $(10)_{Pt}$ is still visible. In addition, two diffraction peaks stemming from the Ar adlayer can be distinguished. Both peaks are azimuthally sharp and only observed in the $\bar{\Gamma}\bar{M}$ azimuth of the substrate. Thus it can be concluded that the hexagonal Ar adlayer is aligned with respect to the underlying Pt substrate (i.e., $\bar{\Gamma}\bar{M}_{Ar}\equiv\bar{\Gamma}\bar{M}_{Pt}$). The two Ar peaks in Fig. 2 are the first- and second-order $(10)_{Ar}$ and $(20)_{Ar}$ adlayer diffraction peaks. From the angular position and wave vector of the incident He beam, $k_i=5.93$ Å^{-1}, a nearest-neighbor Ar distance (lattice parameter) of $a_{Ar}=3.81$ Å is obtained.

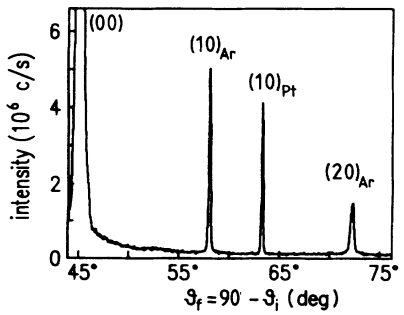

FIG. 2. Polar He diffraction profile along the $\bar{\Gamma}\bar{M}_{Pt}$ azimuth from a 0.3-ML Ar adlayer physisorbed on Pt(111). He beam energy 18.3 meV, surface temperature $T=25$ K.

Figure 3 shows a series of polar profiles of the $(10)_{Ar}$ diffraction peak recorded at 25 K for different coverages. The sequence is characteristic of a first-order phase transition from a structure with a lattice parameter $a_{Ar}=3.81$ Å ($Q=1.90$ Å^{-1}) to one with $a_{Ar}=3.70$ Å ($Q=1.96$ Å^{-1}), below and above 0.75 ML, respectively: The location of the two peaks remains unchanged during the transition; only the relative population of the two structures changes in the region where both phases coexist.

It should be pointed out here that the coverage regime in which both phases coexist largely depends on the preparation of the Ar adlayer. If Ar is adsorbed at low temperature without annealing, the compressed Ar phase ($a_{Ar}=3.70$ Å) is observed already at relatively low coverage ($\Theta\sim0.4$ ML); however, annealing the adlayer at 30–35 K transforms the structure into an expanded phase ($a_{Ar}=3.81$–3.84 Å) if the total Ar coverage lies below ~0.7 ML and into the compressed phase if

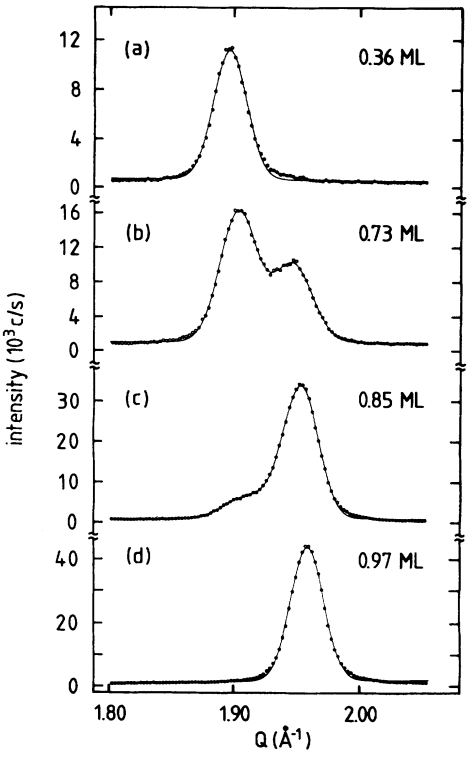

FIG. 3. Polar profiles of the $(10)_{Ar}$ diffraction peak for different Ar coverages. Other experimental parameters as in Fig. 2. The solid lines through the data are best fits using Gaussian line shapes.

$\Theta \gtrsim 0.8$ ML. We interpret this result as being due to local fluctuations in the 2D spreading pressure and island size, which occur in the nonequilibrium Ar adlayer obtained by adsorbing at low surface temperature. Annealing the adlayer reduces these fluctuations, thereby narrowing the phase-coexistence region.

In the following we will address the question concerning the nature of the two Ar phases (below and above the transition), in particular, whether we are dealing with commensurate or HOC phases rather than with "floating" incommensurate phases. For this purpose we have performed thermal-expansion measurements and looked for superlattice diffraction patterns in the two phases; i.e., we have applied the two criteria described in Sec. I by means of which one can distinguish HOC from incommensurate phases.

As a result, the high-coverage Ar phase with an interatomic distance of $a_{\mathrm{Ar}} \simeq 3.70$ Å turns out to be a HOC phase: The thermal expansion of this phase is shown in Fig. 4. Here the Ar lattice parameter as obtained from the position of the first-order Ar diffraction peak is plotted as a function of surface temperature. Obviously, the lattice parameter of the high-coverage Ar phase is—like the one of the Pt substrate—constant within experimental error between 18 and 33 K. As a reference, the thermal expansion of bulk argon[18] is also indicated in Fig. 4 (dashed line). By comparing the experimental data for $T < 33$ K with this dashed curve, it is evident that the thermal expansion of the Ar adlayer is not compatible with that expected for an incommensurate floating phase, but instead corresponds to a structure locked to the Pt(111) substrate.

Another interesting feature in Fig. 4 is the sudden increase of the lattice parameter above $T \simeq 33$ K. Apparently, the high-coverage Ar phase is stable only below $T \sim 33$ K. Above this temperature the thermally induced strain drives the Ar adlayer out of registry (Ar desorption can be detected only above 40 K). We hope this will encourage model calculations and/or molecular-dynamics simulations of the Ar/Pt(111) system.

For an additional check of the high-order commensurate nature of the high-coverage Ar phase and in order to get direct information on the size of the commensurate unit cell, we have searched for superstructure peaks in the He diffraction pattern (the second criterion mentioned above). Figure 5 shows a polar diffraction scan for this high-coverage Ar phase ($\Theta = 0.91$ ML) along the $\bar{\Gamma}\bar{M}$ direction. Indeed, between the specular (0 0) and the first-order Ar diffraction peak $(1\,0)_{\mathrm{Ar}}$, two additional diffraction features are clearly visible at about $\frac{1}{3}$ and $\frac{2}{3}$ of the first-order Ar reciprocal lattice spacing $Q = 1.96$ Å^{-1}. These two peaks are absent in the low-coverage phase. Note that the intensity of the $(\frac{1}{3}\,0)_{\mathrm{Ar}}$ peak in Fig. 5 is only about 5% of the $(1\,0)_{\mathrm{Ar}}$ diffraction-peak height. Yet this intensity ratio is the highest we could achieve. It has been obtained by annealing the high-coverage Ar phase at ~ 35 K and allowing for long equilibration times up to 1 h at low surface temperature (20–25 K).

From the $\frac{1}{3}$ and $\frac{2}{3}$ on-axis position of the superstructure diffraction peaks, it follows that the Ar commensurate superstructure unit cell is aligned and has a lateral periodicity d of 3 times the Ar interatomic distance, i.e., $d = 3 \times 3.70$ Å $= 11.10$ Å.[19] This periodicity must correspond to an integer multiple of the Pt(111) lattice parameter since the Ar superstructure unit cell is commensurate with the substrate. With the known lattice parameter $a_{\mathrm{Pt}} = 2.77$ Å, there is only one possibility, namely, that d is equal to 4 times the Pt interatomic lattice spacing $4 \times a_{\mathrm{Pt}} = 11.08$ Å. With the assumption that one of the two types of threefold-hollow (hcp or fcc) site is the energetically favored adsorption site for a single reference Ar atom, every third Ar atom along any direction occupies the fourth equivalent preferential Pt(111) threefold-hollow adsorption site.[20]

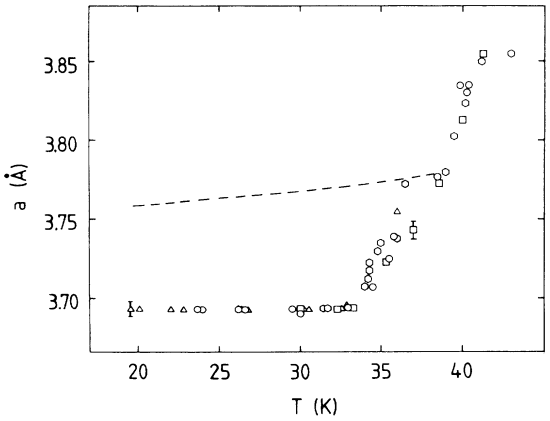

FIG. 4. Lattice parameter of the Ar monolayer as a function of surface temperature. Different symbols correspond to Ar adlayers with different total coverage in the range $0.85 \leq \Theta \leq 1$ ML. The dashed line indicates the thermal variation of the interatomic distance in bulk argon (Ref. 18). This should be very close to the thermal expansion of an incommensurate overlayer as shown in the case of Kr/Pt(111) (Ref. 10).

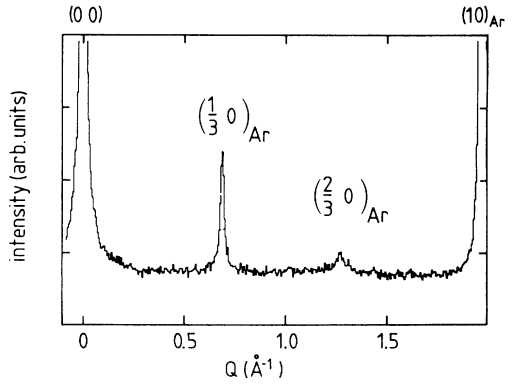

FIG. 5. Polar diffraction profile of the Ar monolayer ($\Theta = 0.91$ ML) on Pt(111). From the position of the superstructure diffraction peaks $(\frac{1}{3}\,0)_{\mathrm{Ar}}$ and $(\frac{2}{3}\,0)_{\mathrm{Ar}}$, the actual nature of the high-coverage Ar HOC phase can be determined: The commensurate unit cell is aligned with the substrate, and its length is 3 times the Ar interatomic distance; $d = 3 \times a_{\mathrm{Ar}} = 4 \times a_{\mathrm{Pt}} = 11.08$ Å.

We may thus conclude that the high-coverage Ar phase forms a $(4\times4)R0°$ high-order commensurate structure, characterized by a $(4\times4)R0°$ unit cell occupied by $3\times3=9$ Ar atoms. A schematic representation of this structure is given in Fig. 6 (here the arrangement of the atoms in the Ar lattice is assumed to be rigid). It should be pointed out that, in addition to the Ar atoms on the corners of the $(4\times4)R0°$ unit cell, another atom is located on a threefold-hollow site, which, however, is of hcp type if the corner sites are fcc sites or vice versa. Simple counting in Fig. 6 shows that two out of nine Ar atoms are located in high-coordination fcc and hcp sites. Comparison of these results with those obtained for the Kr monolayer on Pt(111) (Ref. 10) shows that the number of adatoms in high-coordination threefold-hollow sites is larger for the $Ar(4\times4)R0°$ HOC phase (22%) than for the $Kr(5\times5)R0°$ HOC phase (17%). However, the Kr HOC phase is thermally stable up to at least 50 K, whereas the Ar HOC phase is stable only below 33 K. At first sight this seems to conflict with the "stronger" locking of the Ar phase and the expected larger relative corrugation for Ar as compared to Kr. However, the importance of thermal fluctuations on the stability of the HOC phases is given by the relative contribution of the entropy term to the total free energy of the adsorption system. For a realistic comparison the temperature should therefore be scaled relative to the total adsorption energy of the corresponding species, i.e., to the latent heat of adsorption, which has been measured to 154 meV for Kr/Pt(111) (Ref. 2) and 96 meV for Ar/Pt(111).[21] By scaling with the ratio of these binding energies, a temperature of 33 K in the case of Ar should be compared to 53 K for Kr. Strain effects may also play an important role: While the nearest-neighbor distance in the Kr HOC phase lies very close to the Kr bulk value,[10] the $Ar(4\times4)R0°$ phase appears to be compressed (cf. Fig. 4). The resulting strain in the Ar HOC phase is even enhanced with increasing temperature and will eventually drive the Ar adlayer out of registry.

We will now focus on the low-coverage Ar phase observed at Ar coverages $\Theta\lesssim0.75$ ML. The characterization of this phase has proven to be much more difficult than for the high-coverage $(4\times4)R0°$ HOC phase.

In analogy with the experiments described above for the high-coverage Ar phase, we have measured the thermal expansion and searched for additional superlattice diffraction peaks also in the low-Ar-coverage regime. In these experiments the low-coverage Ar phase ($\Theta_{Ar}\simeq0.36$ ML) was prepared by dosing Ar at low surface temperature (20–25 K) and successively briefly annealing the adlayer. Depending on the annealing temperature and annealing time, either an Ar lattice parameter of (1) $a_{Ar}\simeq3.81$ Å or (2) a slightly larger value of $a_{Ar}\simeq3.83$ Å was obtained. This is also reflected in the thermal-expansion data summarized in Fig. 7. Starting with phase (1) ($a_{Ar}=3.81$ Å), the Ar lattice parameter remains unchanged within experimental error up to a surface temperature of about 30 K. By heating to higher temperatures, the Ar adlayer eventually expands into a second phase [phase (2)] ($a_{Ar}=3.83$ Å). Cooling this phase again to 20 K leaves the Ar adlayer in the expanded phase (2). Increasing the surface temperature to still higher values leads to further expansion of the Ar adlayer beyond $a_{Ar}=3.83$ Å. Again, the expansion is not completely reversible. Obviously, once the expanded phase (2) is reached upon cooling, the Ar adlayer does not seem to compress further. This behavior could, in principle, be accounted for by the desorption of part of the Ar overlayer: When the adlayer is heated, the particle density could decrease as a consequence of desorption and the adlayer might lock into a less compressed phase, which would correspond to the equilibrium phase at this lower coverage. However, we have pointed out earlier that desorption over the time scale of the experiments is only observed above 40 K. Furthermore, a succession of various equilibrium phases with coverage should be observable as jumps or at least a shift in the peak position in the diffraction profiles taken as a function of coverage (cf.

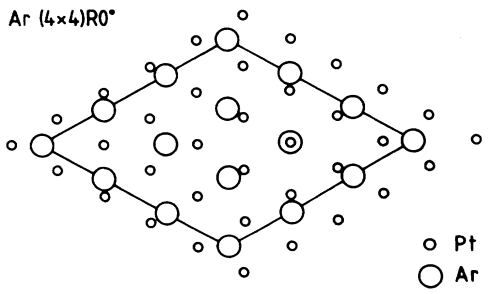

FIG. 6. Schematic representation of the $Ar(4\times4)R0°$ high-order commensurate structure on Pt(111). Small and large circles correspond to Pt and Ar atoms, respectively. The solid line indicates the $(4\times4)R0°$ commensurate unit cell.

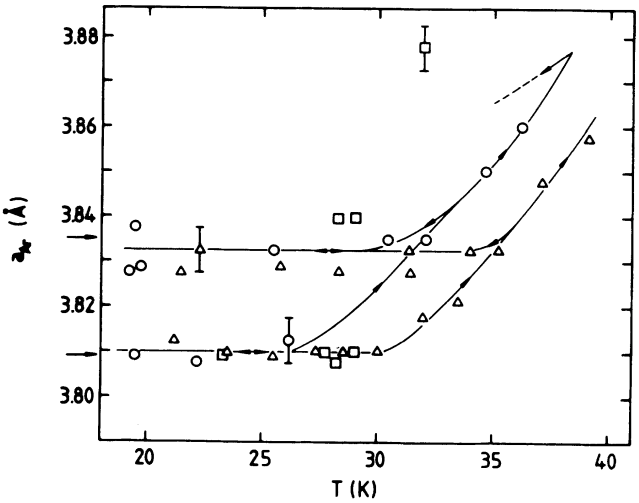

FIG. 7. Thermal expansion of the Ar adlayer in the low-coverage regime ($\Theta\simeq0.36$ ML) The lines through the data demonstrate the irreversibility of the expansion. Different symbols correspond to different measuring runs. The two lattice parameter values marked by the arrows correspond to the theoretical Ar interatomic distance in the $(11\times11)R0°$ ($a_{Ar}=3.809$ Å) and the $(18\times18)R0°$ ($a_{Ar}=3.835$ Å) high-order commensurate phase, see Table I.

Fig. 3). However, even at coverages below 0.36, the Ar phase (1) with $a_{Ar}=3.81$ Å can be obtained. This demonstrates that the formation of one or the other low coverage phase is not a matter of overall density and thus that the behavior in Fig. 7 is not due to desorption. One would also expect the thermal-expansion curves for different experimental runs (indicated by different symbols in Fig. 7) to be different because of variations in initial coverage and thermal treatment. This does not seem to be the case. Therefore, we believe that the most likely reason for the observed behavior is the metastability of the HOC phases: Once the Ar phase is "trapped" upon cooling in one HOC phase, it cannot compress further because of its being kinetically hindered. Such a behavior is indeed expected for locked (HOC) phases since it takes a finite energy to displace a commensurate phase.

In conclusion, an irreversible thermal expansion of the low-coverage Ar phase is observed. However, this expansion appears to proceed in discrete steps, favoring in particular two Ar adlayer structures characterized by lattice parameters $a_{Ar}\simeq 3.81$ and 3.83 Å, respectively. The irreversibility of the expansion after surpassing 30 K, the preferential organization into phases (1) and (2), as well as the lack of thermal expansion between 18 and 30 K evidenced in Fig. 7, clearly shows that the Ar adlayer is locked to the underlying substrate. This behavior is indicative of further registered HOC phases in the Ar adlayer structure. It is apparent from Fig. 7 that the thermal stability of the low-coverage Ar registered phases is much smaller than that of the $(4\times4)R0°$ HOC phase. That there are indeed discrete jumps in the thermal variation of the Ar lattice parameter as expected for a transition between phases in registry with the substrate is demonstrated in Fig. 8. Here the polar diffraction profiles recorded from an Ar adlayer in the low-coverage phase ($\Theta=0.36$ ML) for different surface temperatures are shown. The three spectra [Figs. 8(a)–8(c)] indicate the coexistence and discontinuous transition between (partially) locked structures, in this case characterized by lattice parameters $a_{Ar}\simeq 3.81$, 3.84, and 3.88 Å.

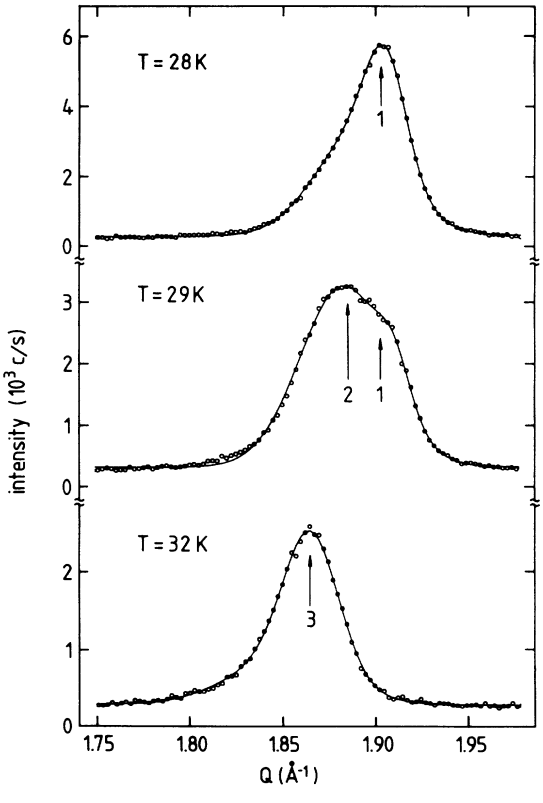

FIG. 8. Polar He diffraction profiles of the $(1\,0)_{Ar}$ peak in the low-Ar-coverage regime ($\Theta=0.36$ ML) at different surface temperatures. The sequence (a)–(c) demonstrates the discontinuous transition between different Ar phases locked to the Pt(111) substrate: (1) $a_{Ar}=3.81$ Å ($Q=1.905$ Å^{-1}), (2) $a_{Ar}=3.84$ Å ($Q=1.890$ Å^{-1}), and (3) $a_{Ar}=3.88$ Å ($Q=1.870$ Å^{-1}). These spectra were recorded with a He beam energy of 17.5 meV. The solid lines are again best-fit Gaussians.

Unfortunately, no additional Ar superlattice diffraction patterns could be observed. Therefore, the cross-check for the locked phases in the low-Ar-coverage regime being high-order commensurate phases could not be given. Since the superstructure He diffraction peaks of the $(4\times4)R0°$ HOC phase are already very weak, this is perhaps not too surprising. A larger commensurate superstructure unit cell, leading to a smaller buckling of the adlayer and a possible weaker ordering of these HOC phases, might deteriorate the diffraction intensity of the superlattice diffraction spots below the experimental detection limit.

Nevertheless, it is worthwhile to consider possible high-order commensurate structures on the Pt(111) substrate and to compare them to the locked phases observed in our experiment. Table I gives a list of all hexagonally aligned HOC structures with a realistic interatomic distance a_{Ar} between 3.6 and 3.9 Å and a size of the unit commensurate unit cell of $d\lesssim 60$ Å. Those HOC structures with small unit cells (i.e., small d) are expected to be the most stable ones. In fact, the first favorite (No. 1 in Table I) is the $(4\times4)R0°$ HOC structure with a periodicity $d=11.08$ Å, which is observed experimentally and has been shown to be stable over a large temperature range. The most interesting result apparent from Table I is the fact that the locked phases observed in the experiment with $a_{Ar}=3.81$ and 3.83 Å compare surprisingly well with HOC structure Nos. 3 and 7 in Table I, which are the two most favored HOC phases in the range of interest from $a_{Ar}=3.8$ to 3.85 Å. This provides strong evidence for the high-order commensurate nature of the locked "metastable" phases (1) and (2), which would then be identified as the $(11\times11)R0°$ ($a_{Ar}=3.809$ Å) and the $(18\times18)R0°$ ($a_{Ar}=3.835$ Å) HOC phase, respectively. Comparing the experimental results with Table I, we can make an even stronger statement: Within the range of the experimentally observed nearest-neighbor Ar distances, all the predicted most stable HOC phases were actually observed in the experiment with the exception of the $(15\times15)R0°$ HOC phase with $a_{Ar}=3.777$ Å and the $(19\times19)R0°$ phase with $a_{Ar}=3.759$ Å. In fact, the continuous increase of the lattice parameter above the critical temperature of 33 K in Fig. 4 is likely to be the expansion of a constrained incommensurate phase. It is, indeed, hard to imagine that another HOC phase (neces-

TABLE I. Complete list of the hexagonally aligned HOC structures for the Ar/Pt(111) system leading to an Ar interatomic distance between $a_{Ar}=3.6$ and 3.9 Å listed in the order of the (linear) size d of their commensurate unit cells for $d<60$ Å. The HOC structures are characterized by the rational number of Ar to Pt atoms (second column). The denominator gives the periodicity of the HOC phase in units of the Pt(111) lattice spacing; the numerator squared yields the number of Ar atoms per unit cell. For instance, 3:4 refers to the $(4\times4)R0°$ HOC phase with $3^2=9$ Ar atoms per unit cell (see Fig. 6).

No.	Structure	Interatomic Ar spacing a_{Ar} (Å)	Commensurate unit cell d (Å)
1	3:4	3.693	11.08
2	5:7	3.878	19.39
3	8:11	3.809	30.47
4	10:13	3.601	36.01
5	11:15	3.777	41.55
6	13:17	3.622	47.09
7	13:18	3.835	49.86
8	14:19	3.759	52.63
9	16:21	3.636	58.17

sarily with a larger unit cell) could be stable beyond the critical temperature of the energetically favored $(4\times4)R0°$ phase. The fact that we do not observe distinct "steps" in the expansion curve in Fig. 4 indicates that those HOC phases with a_{Ar} between 3.69 and 3.81 Å are not stable over a finite temperature range above 33 K. This, again, demonstrates the extreme thermal stability of the $(4\times4)R0°$ phase. Only at low coverage, where the $(4\times4)R0°$ phase is not present, is it possible to observe the less stable HOC phases.

IV. CONCLUSIONS

A *series* of HOC phases and their mutual phase transitions have been observed in a physisorption system, and we might classify the structural phase transitions of the Ar monolayer as an (incomplete) *devil's staircase.* The dominance of locked HOC structures in the Ar monolayer on Pt(111) is naturally explained within the simple model of competing interactions, corrugation u_c versus lateral attraction h. Because of the decreasing ratio h/u_c with increasing rare-gas atom size, we expect on the Pt(111) surface a gradual transition from the floating Xe monolayer with its rich diversity of incommensurate domain-wall phases[22] through Kr layers with coexisting incommensurate and HOC locked phases[10] to predominantly locked Ar layers dominated by the registry forces of the substrate. The rare-gas monolayers on the Pt(111) surface thus represented an interesting system with which to study the whole spectrum of phenomena and phase transitions of two-dimensional matter with competing interactions.

*Permanent address: Institut de Physique Expérimentale, EPF Lausanne, PHB-Ecublens, Ch-1015 Lausanne, Switzerland.

[1]G. Dash, *Films on Solid Surfaces* (Academic, New York, 1975); Contemp. Phys. **30**, 89 (1989).

[2]K. Kern and G. Comsa, in *Chemistry and Physics of Solid Surfaces VII,* edited by R. Vanselow and R. F. Howe (Springer, Heidelberg, 1988), p. 65.

[3]E. D. Specht, A. Mak, C. Peters, M. Sutton, R. J. Birgeneau, K. L. D'Amico, D. E. Moncton, S. E. Nagler, and P. M. Horn, Z. Phys. B **69**, 347 (1987).

[4]R. J. Birgeneau and P. M. Horn, Science **232**, 329 (1986).

[5]K. Kern, P. Zeppenfeld, R. David, and G. Comsa, J. Vac. Sci. Technol. A **6**, 639 (1988).

[6]J. Villain and M. B. Gordon, Surf. Sci. **125**, 1 (1983); P. Bak, in *Chemistry and Physics of Solid Surfaces V,* edited by R. Vanselow and R. F. Howe (Springer, Berlin, 1984), p. 317.

[7]P. Bak, D. Mukamel, J. Villain, and K. Wentowska, Phys. Rev. B **19**, 1610 (1979).

[8]K. Kern, R. David, P. Zeppenfeld, R. L. Palmer, and G. Comsa, Solid State Commun. **62**, 391 (1987); J. Cui, C. S. Fain, H. Freimuth, H. Wiechert, P. Schildberg, and H. J. Lauter, Phys. Rev. Lett. **60**, 1848 (1990).

[9]S. Aubry, in *Solitons and Condensed Matter Physics,* edited by A. R. Bishop and T. Schneider (Springer, Berlin, 1978), p. 264.

[10]K. Kern, P. Zeppenfeld, R. David, and G. Comsa, Phys. Rev. Lett. **59**, 79 (1987).

[11]W. Weimer, K. Knorr, and H. Wiechert, Phys. Rev. Lett. **61**, 1623 (1988); T. Meichel, J. Suzanne, C. Girard, and C. Girardet, Phys. Rev. B **38**, 3781 (1988).

[12]K. S. Liang, K. L. D'Amico, C. H. Lee, and E. Y. Sheu, Phys. Rev. Lett. **65**, 3025 (1990).

[13]W. A. Steele, Surf. Sci. **36**, 317 (1973).

[14]G. Vidali and M. W. Cole, Phys. Rev. B **29**, 6736 (1984).

[15]R. David, K. Kern, P. Zeppenfeld, and G. Comsa, Rev. Sci. Instrum. **57**, 2771 (1986).

[16]B. Poelsema, R. L. Palmer, G. Mechtersheimer, and G. Comsa, Surf. Sci. **117**, 60 (1982).

[17]B. Poelsema and G. Comsa, in *Scattering of Thermal Energy Atoms from Disordered Surfaces,* edited by G. Höhler and E. A. Niekisch (Springer, Heidelberg, 1989).

[18]M. L. Klein, G. K Horton, and J. L. Feldman, Phys. Rev. **184**, 968 (1969).

[19]The position of the $(\frac{1}{3}\,0)_{Ar}$ superlattice diffraction peak appears to be shifted slightly toward higher Q values. Although this may be an experimental artifact it could also be due to an additional fine structure, as, for instance, a domain-wall pattern, within the HOC Ar phase.

[20]According to a recent *ab initio* cluster calculation of J. Müller [Phys. Rev. Lett. **65**, 3021 (1990)], however, the on-top loca-

tion is the energetically most favorable adsorption position for a Xe atom on a Pt(111) surface. This might equally hold for the Ar atom on this surface. Nevertheless, the actual binding site has no consequences for the following discussion, and we assume for simplicity the hollow sites to be the favorable adsorption sites.

[21]P. Zeppenfeld, K. Kern, and U. Becher (unpublished).
[22]K. Kern, Phys. Rev. B **35**, 8265 (1987).